UV and UV/H$_2$O$_2$ treatment of methylisoborneol (MIB) and geosmin in water

Erik J. Rosenfeldt, Barbara Melcher and Karl G. Linden

ABSTRACT

The presence of taste and odour-causing compounds in water can lead consumers to perceive the water as unsafe and thus is a great concern for water utilities. This study examined the effectiveness of direct ultraviolet (UV) photolysis and the UV/hydrogen peroxide (H$_2$O$_2$) advanced oxidation process (AOP) for removing methylisoborneol (MIB) and geosmin from raw source water and treated water. Low Pressure (LP) and Medium Pressure (MP) direct UV photolysis removed 10% and 25–50% of the compounds by 1000 mJ cm^{-2} UV fluence, respectively. The addition of H$_2$O$_2$ created advanced oxidation conditions, and oxidized greater than 70% of these compounds at a UV fluence of 1000 mJ cm^{-2}. MP UV + H$_2$O$_2$ was consistently faster than LP UV + H$_2$O$_2$ for MIB oxidation, but water quality affected both of the UV + H$_2$O$_2$ AOPs. The UV + H$_2$O$_2$ AOP oxidation of these taste and odour contaminants in natural waters was effectively modelled using the steady state OH radical concentration model. Finally, electrical energy per order (E$_{EO}$) values for oxidation of MIB and geosmin were determined for a model UV reactor, and indicated that the UV + H$_2$O$_2$ AOP requires less than 5 kWh of UV energy to oxidize 90% of MIB or geosmin in 1,000 gallons (3,785 liters) of clearwell or raw blend water, corresponding to a cost of less than US$0.35 per 1000 US gallons (3,785 liters).

Key words | advanced oxidation, kinetics, photolysis, taste and odour, ultraviolet

Erik J. Rosenfeldt
Karl G. Linden (corresponding author)
Department of Civil and Environmental
   Engineering,
Duke University,
Durham, NC 27708,
USA
Tel: 919-660-5196
Fax: 919-660-5219
E-mail: *kglinden@duke.edu*

Barbara Melcher
Camp Dresser & McKee Inc,
Chicago, IL60606,
USA

NOMENCLATURE

λ	wavelength (nm)
k'	pseudo-first order rate constant (s^{-1})
k'_d	direct photolysis pseudo-first order rate constant (s^{-1})
k'_i	indirect photolysis pseudo-first order rate constant (s^{-1})
$k_{C,OH}$	second order rate constant for the reaction between OH radical and a compound 'C' (M^{-1} s^{-1})
$k_s(\lambda)$	energy absorbed by hydrogen peroxide (Es mol^{-1} s^{-1})
$\Sigma k_{S,OH}[S]$	sum of the scavenging (s^{-1})
$N_o(\lambda)$	photon fluence rate (mEs cm^{-2} s^{-1})
$\varepsilon(\lambda)$	molar absorption coefficient (M^{-1} cm^{-1})
$a(\lambda)$	UV absorbance (cm^{-1})
z	pathlength (cm)

C_f	final concentration (M)
C_i	initial concentration (M)
t	time (s)
E_{EO}	electrical energy per order (kWh per 1000 US gallons) (3,785 liters)
P	power (kW)
V	volume (l)
E'_{avg}	average UV fluence rate (mW cm^{-2})

INTRODUCTION

The presence of foul tastes and odours in source water is of major concern to the drinking water treatment industry. Caused by the presence of chemicals in the water, these earthy, musty, chlorinous, sour, metallic, fishy, medicinal and chemical tastes or odours can lead to perceptions by consumers that the water is unsafe to drink, even though it

meets guidelines for regulated constituents. Musty and earthy odours are two of the most frequently reported complaints to utilities (Suffet *et al.* 1996). Two compounds commonly associated with earthy and musty odours in surface waters are 2-methylisoborneol (MIB) and geosmin. These compounds are metabolites mainly from blue-green algae and actinomycetes and can be detected in most source waters and drinking water at low concentrations. The average threshold odour concentration for these compounds is approximately $10\,ng\,l^{-1}$ (Suffet *et al.* 1999), and can be even lower depending on the taste and odour sensitivity of the individual.

Removal of MIB and geosmin has proved difficult for the water treatment industry. Studies have shown that the typical treatment trains, including coagulation, flocculation, filtration and addition of chlorine are ineffective in removing some soluble odour-causing chemicals, including MIB and geosmin (Hargesheimer & Watson 1996; Bruce *et al.* 2002). At least one study has found removal by bioreactors to be ineffective, and concluded that biodegradation could not be used as a primary removal method for taste and odour compounds in drinking water (Huck *et al.* 1995). Activated carbon has been used successfully to remove taste and odours from source waters. Addition of powdered activated carbon (PAC), and treatment by granular activated carbon (GAC) filters has been shown to reduce concentrations of taste and odour-causing compounds to levels below threshold odour concentrations (Hargesheimer and Watson 1996; Gillogly *et al.* 1999; Crozes *et al.* 1999; Bruce *et al.* 2002).

Oxidation techniques have been utilized for taste and odour removal with mixed success. Typical oxidative techniques utilized include the addition of chlorine (Cl$_2$), chlorine dioxide (ClO$_2$), ozone (O$_3$), or potassium permanganate (KMnO$_4$). Lalezary *et al.* (1986) showed that these four oxidative techniques were all effective in removing taste and odour-causing chemicals, but MIB and geosmin were typically the least efficiently oxidized. This is due to the resistance to oxidative treatments typically displayed by tertiary alcohols. Relative efficiencies of the treatments for MIB and geosmin oxidation were found to be ClO$_2$ > O$_3$ > Cl$_2$ > KMnO$_4$ in pre-stripped, organically pure water at low oxidant doses. However, Glaze *et al.* (1990) found that ozone oxidized MIB and geosmin in Colorado river water much faster than HOCl, ClO$_2$, KMnO$_4$ or H$_2$O$_2$ alone, and

postulated that the organics present in the natural water were facilitating ozone decomposition to OH radical, and advanced oxidation of MIB and geosmin.

Because of the inefficiencies of destruction by traditional water treatment processes, including oxidation under certain conditions, alternative methods of taste and odour removal or destruction are being examined. Advanced oxidation processes have shown promise in the destruction of taste and odour-causing compounds. Studies involving the use of ozone, hydrogen peroxide in combination with ozone, ozone with UV irradiation, and titanium dioxide (TiO$_2$) with UV irradiation exhibited destruction of MIB and geosmin to levels below the threshold odour concentration (Lalezary *et al.* 1986; Glaze *et al.* 1990; Ferguson *et al.* 1990; Koch *et al.* 1992; Lawton *et al.* 2003).

Two treatment process that have not been studied in detail for destruction of taste and odour-causing compounds are UV based direct photolysis and the UV + hydrogen peroxide (H$_2$O$_2$) advanced oxidation process (AOP). In batch tests using a 1 kW medium pressure (MP) UV lamp, MP UV was found to have little effect on the concentration of geosmin present in solution (Andrews *et al.* 1995). However, addition of 5 or $25\,mg\,l^{-1}$ of H$_2$O$_2$ resulted in rapid oxidation of geosmin. It was also found that the electrical energy required to reduce the concentration of geosmin in 1,000 US gallons (3,785 litres) by an order of magnitude was relatively economical. This study suggested that UV + H$_2$O$_2$ AOP may be effective for treatment of taste and odour-causing compounds. Direct low pressure (LP) and MP UV photolysis, as well as LP and MP UV + H$_2$O$_2$ AOP, were compared for removal of MIB and geosmin in raw source water and finished water, utilizing environmentally relevant spiked levels of MIB and geosmin.

MATERIALS AND METHODS

Chemicals/waters

MIB and geosmin in methanol were purchased from Wako Chemical (Osaka, Japan) and diluted to a stock concentration of $950\,\mu g\,l^{-1}$ in ultrapure water; 30% hydrogen peroxide (J.T. Baker, Phillipsburg, New Jersey) was used to spike at $mg\,l^{-1}$ levels. Bovine liver catalase (Sigma-Aldrich

Corporation) was used to quench any residual H$_2$O$_2$ following exposures (Liu *et al.* 2003). Test water samples were shipped from the Jardine Water Purification Plant (JWPP) in Chicago, Illinois, to the Department of Civil and Environmental Engineering at Duke University and stored at 4°C until experiments were performed. Samples from two points in the process train of the water treatment plant were collected: raw blend water, made up of 60% water from the shore, and 40% water from the cribs (large underwater intake tunnels approximately 3 kilometers into lake Michigan), and combined filter effluent (composite sample from all eight clearwells). All samples were collected by the control lab in the JWPP.

UV reactors

Irradiation by a 1 kW medium pressure UV lamp (Hanovia Co., Union, New Jersey) was performed using a bench-scale collimated beam UV reactor provided by Calgon Carbon Corporation (CCC, Pittsburgh, Pennsylvania) modified at Duke University. Irradiation by a low pressure UV lamp was performed using another bench-scale collimated beam UV reactor fitted with four 15-W low-pressure UV lamps. Figure 1 shows a typical 'collimated beam' UV system consisting of the light source, a 'collimating' device, a support stand, and an exposure control system comprising a manual (LP UV) or pneumatic (MP UV) shutter. A UV radiometer and detector (International Light Inc., Model 1700/SED 240/W) calibrated traceable to standards at the National Institute of Standards and Technology (NIST) at 2 nm intervals in the range of 200 to 400 nm was used to measure UV irradiance at the surface of the test water.
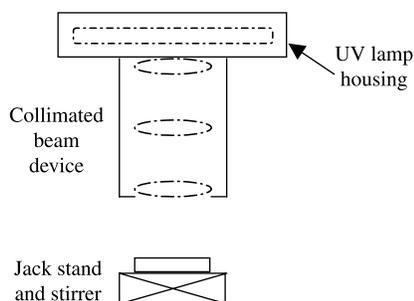
Figure 1 │ Basic 'collimated beam' device used in taste and odour UV testing.

UV fluence calculation

One of the most important concepts in UV photochemistry involves the determination of delivered UV fluence (also termed 'UV dose' in some literature). UV fluence (mJ cm^{-2}, where J = W s) was calculated as the average irradiance multiplied by the exposure time. The average UV irradiance in the completely mixed sample was determined from the incident irradiance, UV absorbance and sample depth using an integrated form of the Beer-Lambert law and calculated using an MS Excel spreadsheet (as per Bolton and Linden 2003). Incident UV irradiance (mW cm^{-2}) was measured with a radiometer at the surface of the liquid suspension. All UV fluence values reported for the MP UV source were calculated as a function of the entire lamp output between 200 and 300 nm. Samples were exposed to UV light for specific time intervals using a shutter system above the reaction vessel. The exposure time (seconds) necessary was determined by dividing the desired UV fluence (mJ cm^{-2}) by the average UV fluence rate (mW cm^{-2}). UV absorbance (200–300 nm) of the spiked test water was measured in a spectrophotometer (Cary 100 bio-spectrophotometer, Varian, Houston, Texas).

Analytical methods

MIB and geosmin analysis

Analysis for MIB and geosmin was performed by Environmental Health Laboratories, South Bend, Indiana, according to Standard Method 6040C, purge and trap, followed by GC/MS detection. The detection limit for each compound was 5 ng l^{-1}.

H$_2$O$_2$ concentration determination

Hydrogen peroxide concentration was determined using the I$_3^-$ method (Ghormley method) outlined in Klassen *et al.* (1994). This method is accurate to H$_2$O$_2$ concentrations as low as 1 μM, and utilizes a colour change that occurs when H$_2$O$_2$ reacts with KI in a buffered solution containing ammonium molybdate as a catalyst.

Water quality parameters

Turbidity was analysed using a Hach 2100 N Turbidimeter (Hach Corp., Loveland, Colorado). Temperature and pH were measured with the appropriate calibrated probes. Alkalinity was measured according to Standard Methods 2320 B. Total organic carbon (TOC) was measured in accordance with Standard Method 5310 A (combustion and detection method) (Tekmar Dohrmann Apollo 9000 Total Carbon analyser). Water quality parameters of interest are presented in Table 1.

UV exposure procedure

MIB and gesomin was spiked from the $950\,\mu g\,l^{-1}$ stock into raw blend or clearwell water to an initial concentration of approximately $25\,ng\,l^{-1}$ MIB and $10\,ng\,l^{-1}$ geosmin. These concentrations correspond to typical concentrations found at the JWPP during a taste and odour event. Samples (120 ml) were measured into 70×50 mm flat bottom Pyrex petri dishes, and then spiked with H_2O_2 at concentrations of 0, 2 or $7.5\,mg\,l^{-1}$. Table 2 displays the overall experimental plan. A small stir bar was added and mixing began at a rate that allowed for good mixing, but disturbed the surface of the water minimally.

Samples were taken for absorption measurement (0.7 ml), and initial H_2O_2 analysis (0.1 – 0.2 ml). The waters were then irradiated in the MP or LP UV bench scale system for the proper times corresponding to the desired UV fluence, and a final H_2O_2 sample was taken for analysis. After irradiation, $0.2\,mg\,l^{-1}$ catalase was added to quench the remaining H_2O_2, and samples were taken to fill a 45 ml glass vial with no headspace. Catalase was added at this level to quench any remaining hydrogen peroxide. Liu *et al.* (2003) found a rate for the quenching reaction of $0.17\,min^{-1}$. Therefore, the remaining peroxide was removed from the samples in less than 30 minutes. Vials were stored at 4°C, packaged in coolers, and sent to EHL laboratories for analysis.

Because of the volatility of MIB and geosmin, control samples were stirred in the same exposure dishes for times corresponding to the longest UV fluence, but were not exposed to any UV light. Control samples were taken with and without the addition of hydrogen peroxide when applicable to determine if any oxidation was caused by the addition of H_2O_2 alone.

UV/H₂O₂ AOP modelling

To predict the oxidation of MIB and geosmin in water using UV/H₂O₂ AOP, degradation of these species under different

Table 1 │ Water quality parameters of interest; $0\,mg\,l^{-1}$ H₂O₂ testing was performed in the November water, while 2 and $7\,mg\,l^{-1}$ H₂O₂ testing was performed in the July water

Test date	Parameter	Analysis site	Raw blend	Clearwell
July	Turbidity (NTU)	A	2.9	0.16
July	TOC ($mg\,l^{-1}$)	A	2.3	2.2
July	pH	A	8.4	7.6
July	Alkalinity ($mg\,l^{-1}$ as CaCO₃)	A	105	105
November	Turbidity (NTU)	B	7.18	0.103
November	TOC	C	1.7	1.5
November	pH	B	8.03	7.96
November	Alkalinity ($mg\,l^{-1}$ as CaCO₃)	B	105	98

A: Analysed by CDWM, water was dechlorinated using sodium bisulfite prior to testing
B: Analysed at Duke university
C: CDWM (2002)

Table 2 │ Experimental matrix

Water type	Lamp	H₂O₂ added (mg l⁻¹)	UV fluences sampled for MIB/geosmin (mJ cm⁻²)
Raw blend	LP	0	0, 50, 500, 1,000, 1,000 (B)
Raw blend	LP	2.2	0, 50, 150, 300, 500, 1,000, 2,000, 5,000, 5,000 (A), 5,000 (B), 5,000
Raw blend	MP	0	0, 50, 500, 1,000, 1,000 (B)
Raw blend	MP	0	0, 1,000, 2,000, 5,000, 10,000, 10,000
Raw blend	MP	2.93	0, 50, 150, 300, 500, 1,000, 2,000, 5,000, 5,000 (A), 5,000 (B), 5,000
Raw blend	MP	7.2	0, 50, 150, 300, 500, 1,000, 1,000 (B), 1,000, 1,000
Clearwell	LP	0	0, 50, 500, 1,000, 1,000 (B)
Clearwell	LP	2.2	0, 50, 150, 300, 500, 1,000, 2,000, 5,000, 5,000 (A), 5,000 (B), 5,000
Clearwell	MP	0	0, 50, 500, 1,000, 1,000 (B)
Clearwell	MP	2.54	0, 50, 150, 300, 500, 1,000, 2,000, 5,000, 5,000 (A), 5,000 (B), 5,000

A: Blank with H₂O₂
B: Blank without H₂O₂

conditions was modelled using a steady state OH radical concentration assumption, to account for the contribution of the OH radicals to the degradation. Equation (1), from Sharpless and Linden (2003), is the governing rate equation for the UV + H₂O₂ AOP, accounting for the pseudo first order rates of both direct UV photolysis and advanced oxidation.

$$\text{Rate} = -\frac{d[C]}{dt} = k'[C] \tag{1}$$

where, $k' = k'_d + k'_i$

k' is the observed pseudo-first order rate constant (s⁻¹)
k'_d is the measured pseudo-first order direct photolysis rate constant (s⁻¹)
k'_i is the pseudo-first order advanced oxidation rate constant (s⁻¹)

In these modelled cases, the photolysis pseudo-first order rate constant (k'_d) was determined experimentally from the direct UV photolysis experiments. A theoretical estimation of the direct photolysis rate constant could not be made due to the lack of absorption of radiation in the UV range displayed by MIB and geosmin, and the lack of reliable quantum yield data for these contaminants.

To calculate the pseudo-first order rate constant for advanced oxidation, a steady state OH radical concentration assumption was made. By multiplying the second order rate constant $k_{C,OH}$ (M⁻¹ s⁻¹) and this steady state OH radical concentration [OH]ss, the AOP contribution to the observed rate constant is described (Equation 2).

$$k'_i = k_{C/OH}[OH]_{ss} \tag{2}$$

[OH]ss was calculated using Equation (3), as the ratio of the formation of OH radicals to the destruction of the radicals, in accordance with Sharpless and Linden (2003).

$$[OH]_{SS} = \frac{\sum k_s(\lambda)\Phi_{OH}(\lambda)[H_2O_2]}{\sum_i k_{S,OH}[S]_i} \tag{3}$$

where,

$$k_s(\lambda) = \frac{N_o(\lambda)\varepsilon(\lambda)[1 - 10^{-a(\lambda)z}]}{a(\lambda)z} \tag{4}$$

$N_o(\lambda)$: incident photon irradiance (mEs cm⁻² s⁻¹)
$\varepsilon(\lambda)$: decadic molar absorption coefficient of hydrogen peroxide (M⁻¹ cm⁻¹)
$a(\lambda)$: solution absorbance (cm⁻¹)
z: solution depth (cm).

$\Phi_{OH}(\lambda) \approx 1$ mol Es⁻¹ is the quantum yield of OH radical generation through the photolysis of H₂O₂ (Baxendale and Wilson 1957). $\Sigma k_{S,OH}[S]$ is the sum of the product of the concentration of OH radical scavenging species [S] and the second order rate constants of the reaction between the scavenging species and OH radical.

Once these pseudo first order rate constants are determined, destruction of MIB or geosmin as a function of time is calculated by integrating Equation (1) into the form:

$$C_f = C_i e^{-(k'_d + k'_i)t} \tag{5}$$

RESULTS AND DISCUSSION

Volatilization loss

Due to the volatile nature of MIB and geosmin and the potential for volatilization in the open reactor, the MIB and geosmin concentration detected at each dose was corrected by a volatilization factor. To determine this factor, a blank sample, spiked with the same amount of MIB or geosmin as the irradiated sample, was stirred in the dark for the time corresponding to the longest UV fluence. Volatilization loss was considered linear over the irradiation time, and a volatilization factor was calculated as the difference between initial and final concentration of the blank samples, divided by the fluence. This gave a per $mJ\,cm^{-2}$ volatilization loss which could then be applied to correct for volatilization of MIB or geosmin during irradiation. Volatilization losses during the experiments were minimal; the volatilization factor for MIB was $1.54 \times 10^{-3}\,ng\,cm^2\,l^{-1}\,mJ^{-1}$, and that for geosmin $5.72 \times 10^{-4}\,ng\,cm^2\,l^{-1}\,mJ^{-1}$.

Direct UV photolysis: LP and MP

The molar absorption coefficient is a measure of the ability of a compound to absorb UV light. It can be used as a first estimate to determine if a compound will be susceptible to treatment with direct LP or MP UV energy. The Grotthus-Draper law states that only when the radiation is absorbed by the molecule as a result of the interaction between the electromagnetic field associated with the molecule and that

associated with the radiation, can the radiation be effective in producing photochemical changes (Wells 1972).

In the case of MIB and geosmin, the molar absorption coefficient is extremely low at 254 nm, the wavelength emitted by monochromatic, LP UV light. However, below 250 nm, the UV absorption begins to increase significantly. Figure 2 displays the molar extinction coefficients of MIB and geosmin overlain on the emission spectra of MP and LP UV lamps. MIB and geosmin both absorb weakly throughout the UV range, with increased absorbance below 250 nm. Geosmin has greater absorbance than MIB at the low wavelengths. The absorbance properties of the compounds suggest that MP UV lamps will be more effective than LP UV for direct photolysis of MIB and geosmin. Figure 3 displays log reduction of MIB and geosmin as a function of UV fluence in raw blend and clearwell water. These values are shown as log reductions to facilitate a comparison to log reductions of pathogens during UV disinfection. Typical UV disinfection fluences are between 20 and 200 $mJ\,cm^{-2}$ for 4–5 log pathogen reduction.

The observed rate constant for MP UV is at least a factor of 2 greater than LP UV, indicating that UV energy at wavelengths other than 254 nm are more effective for degrading MIB and geosmin. Differences also exist between the raw blend and clearwell waters. The principal water quality parameters that differ between the waters are UV absorbance and turbidity. UV absorbance differences are considered in the fluence calculation, so the difference in turbidity is a possible cause for the differences in direct UV photolysis. The raw blend water had a turbidity of 3.1 NTU,
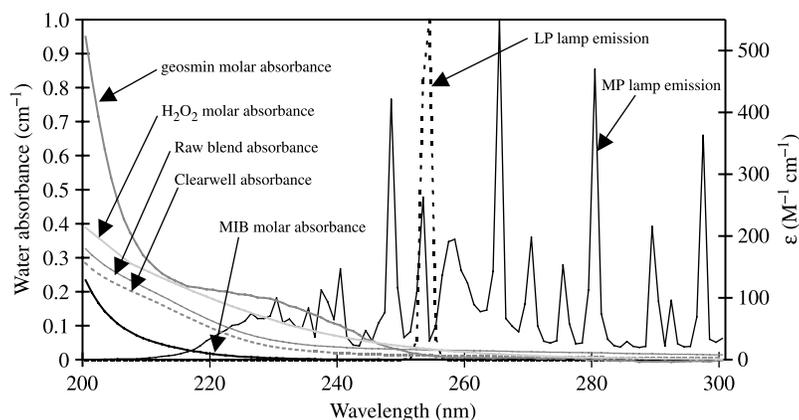
Figure 2 | Molar absorption coefficients for MIB and geosmin, dissolved in lab water (right axis), background absorbance of the tested waters (left axis), and relative emission spectra for the low pressure and medium pressure Hg lamps.
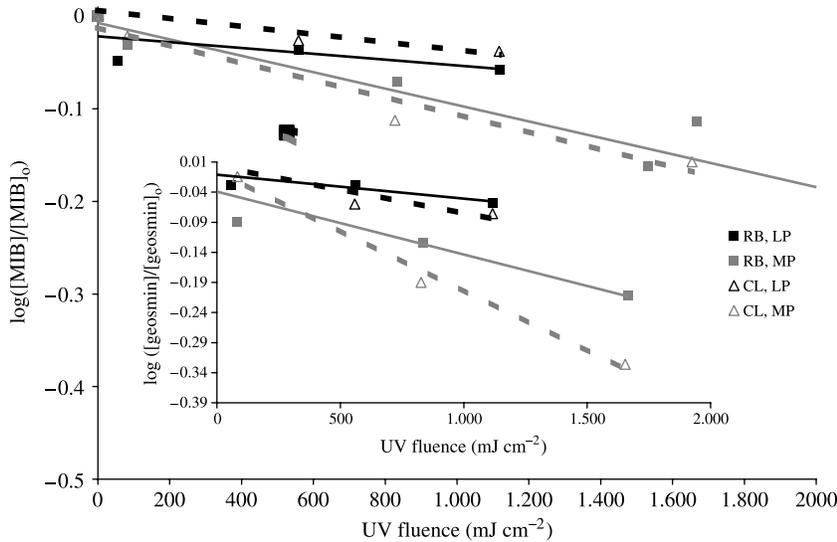
Figure 3 │ Log reduction of MIB and geosmin (inset) as a function of UV fluence in raw blend and clearwell water with LP UV or MP UV.

compared with a value of 0.16 NTU for the clearwell water. If the UV energy is being absorbed, scattered or reflected because of particles in the water, the MIB and geosmin can absorb less of the delivered UV and the destruction process is negatively affected. It has also been shown that light screening by particles can have a negative impact on delivered UV fluence measurements in microbial disinfection (Mamane-Gravetz and Linden 2004).

Advanced oxidation via the UV + H₂O₂ process

Oxidation of MIB and geosmin using UV + H₂O₂ AOP was evaluated for each of the waters. Peroxide was added at low levels to promote hydroxyl radical formation under

irradiation from LP or MP UV sources. As shown in Figure 4, MIB and geosmin removal is enhanced with addition of 2.3 and 7.2 mg l⁻¹ hydrogen peroxide in raw blend water. Pseudo-first order rate constants for all UV + H₂O₂ conditions are displayed in Figure 6.

The observed improvement in destruction with the addition of hydrogen peroxide is due to the fact that the dominant mechanism of treatment when H₂O₂ is present under UV irradiation is hydroxyl radical based advanced oxidation. The highly reactive OH radical species can quickly react with organic species in the water. As H₂O₂ levels are increased, a plateau and eventual decrease in observed rate constant has been shown to occur (Glaze *et al.* 1995; Crittenden *et al.* 1999), but in this study, experiments
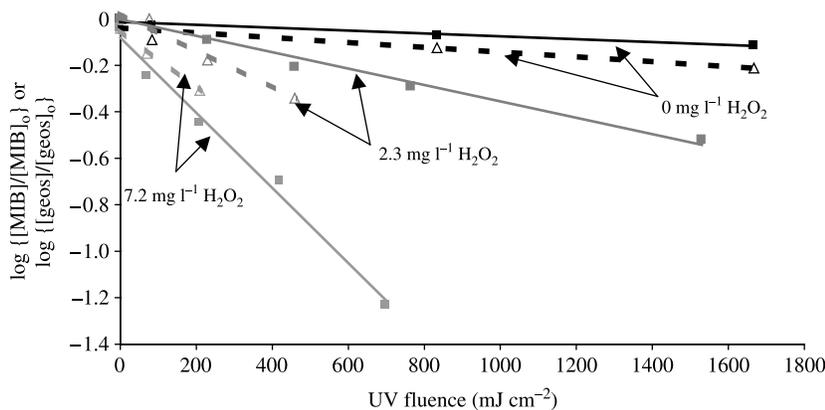
Figure 4 │ Log removal of MIB (solid lines and squares) and geosmin (dashed lines and triangles) in raw blend water using MP UV with and without addition of H₂O₂.

were not performed at high enough peroxide concentrations to observe this effect.

Lamp effects on UV + H$_2$O$_2$ oxidation of MIB and geosmin

Using the MP lamp for UV + H$_2$O$_2$ AOP resulted in a significant increase in the oxidation of MIB (Figure 6) in both clearwell and raw blend water for approximately the same initial peroxide concentration. This is due to the fact that peroxide absorbs UV better at wavelengths below 254 nm (Figure 2), wavelengths emitted by MP UV lamps but not by LP UV lamps. In certain waters with relatively high background absorbance, this effect can be negated by UV light screening, but both waters in this study display relatively low background absorbance below 250 nm (Figure 2). The same effect cannot be discerned from the geosmin data because of the relatively large confidence intervals associated with this data.

Comparison of the UV + H$_2$O$_2$ process in filtered and unfiltered waters

To examine how water quality affects the UV + H$_2$O$_2$ oxidation of MIB and gesomin by the UV/H$_2$O$_2$ process, the destruction of the compounds in clearwell and raw blend water was examined. Table 1 shows the relevant water quality parameters for the clearwell water and the raw blended water samples. Total organic carbon (TOC), pH and alkalinity are used to characterize the OH radical

scavenging ability of the water. Figure 5 displays the destruction of MIB in both clearwell water and raw blended water utilizing the MP UV/H$_2$O$_2$ processes.

In Figure 5, the MP UV + 2.93 mg l^{-1} H$_2$O$_2$ in clearwell water displays destruction kinetics nearly as fast as the MP UV + 7.2 mg l^{-1} H$_2$O$_2$ in raw blend water. This indicates the importance of water quality parameters on the efficiencies of the UV + H$_2$O$_2$ process, as was also noted in the direct UV processes. Differences in OH radical oxidation efficiency in different waters is typically attributed to the presence of radical scavengers such as natural organic matter and carbonate species, but concentrations of these species were similar in both waters. The primary difference in water quality between the raw blend and clearwell waters is turbidity. The relationship between turbidity and the efficiency of the UV + H$_2$O$_2$ process is not well defined. The particles that cause the high turbidity in water can act to 'screen' light from the target compound. In the case of the UV + H$_2$O$_2$ AOP, not as much light is available to H$_2$O$_2$ for OH radical production.

If turbidity-causing particles are organic in nature, they may act as an unaccounted scavenger of OH radicals. Although Koch *et al.* (1992) found that synthetically produced turbidity did not play a role in the destruction of MIB and geosmin by ozone and peroxone AOPs, these findings were qualified by stating that they used inorganic particles to create their turbid conditions. How organic particle turbidity negatively affects UV + H$_2$O$_2$ oxidation of MIB and geosmin is not well understood. These types of water quality consideration will affect the feasible locations of a UV based AOP in a water treatment train.
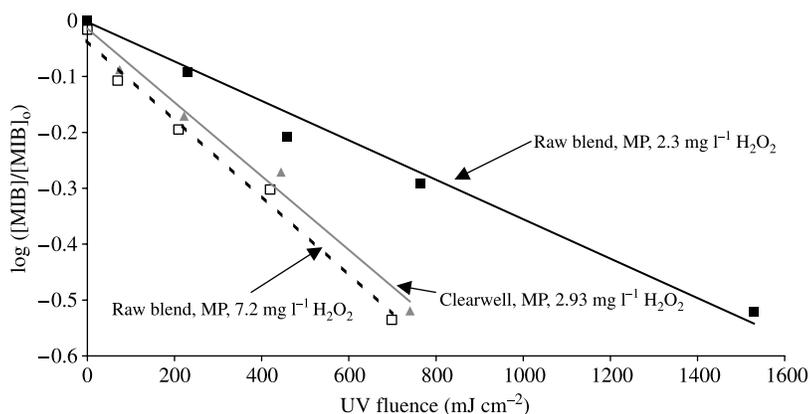

Figure 5 │ Log reduction of MIB by MP UV + 2.3 and 7.2 mg l^{-1} H$_2$O$_2$ (raw blend) and MP UV + 2.93 mg l^{-1} H$_2$O$_2$ (clearwell) processes.

Modelling

The effects of UV lamp type and water quality on the destruction of MIB and geosmin by UV and UV + H_2O_2 processes can be modelled. Using the UV + H_2O_2 model outlined in Equations (1–5), and published OH radical rate constants for MIB, geosmin and the scavengers, predictions of the destruction of the MIB and geosmin were compared with the data. The second order rate constants between the compounds and OH radical are $k_{MIB/OH} = 8.20 \times 10^9 \, M^{-1} s^{-1}$ and $k_{geos/OH} = 1.40 \times 10^{10} \, M^{-1} s^{-1}$ (Glaze *et al.* 1990). Scavengers and corresponding OH radical rate constants used in the model included organic carbon $(2.5 \times 10^4 \, l \, mg^{-1} s^{-1})$ (Larson and Zepp 1988), HCO_3^- $(8.5 \times 10^6 \, M^{-1} s^{-1})$, CO_3^{2-} $(3.9 \times 10^8 \, M^{-1} s^{-1})$, H_2O_2 $(2.7 \times 10^7 \, M^{-1} s^{-1})$ (Buxton *et al.* 1988) and MeOH $(8.9 \times 10^8 \, M^{-1} s^{-1})$ (Notre Dame Radiation Laboratory Chemistry Data Center, www.rcdc.nd.edu/Solnkin2/).

Figure 6 compares the model predicted fluence-based pseudo-first order rate constants (k′ in $cm^2 \, mJ^{-1}$) with observed k′ ($cm^2 \, mJ^{-1}$) values. The model accurately predicts LP UV + H_2O_2 oxidation rates in clearwell and raw blend water with addition of $2.2 \, mg \, l^{-1}$ H_2O_2. For the medium pressure systems, the model predicts well at low H_2O_2, with the exception of geosmin destruction in clearwell water. However, this observed rate constant was calculated using only a few data points and subject to error. As the initial H_2O_2 concentration is raised to $7.2 \, mg \, l^{-1}$ in the MP systems, the model begins to greatly overestimate the destruction of MIB in raw blend water. This may be due to the turbidity issue in the raw blend water, which is not accounted for in the model, although the differences seem dramatic for that effect, and it is not observed at lower initial peroxide concentrations. The model also relies on a calculated OH steady state concentration, which was not
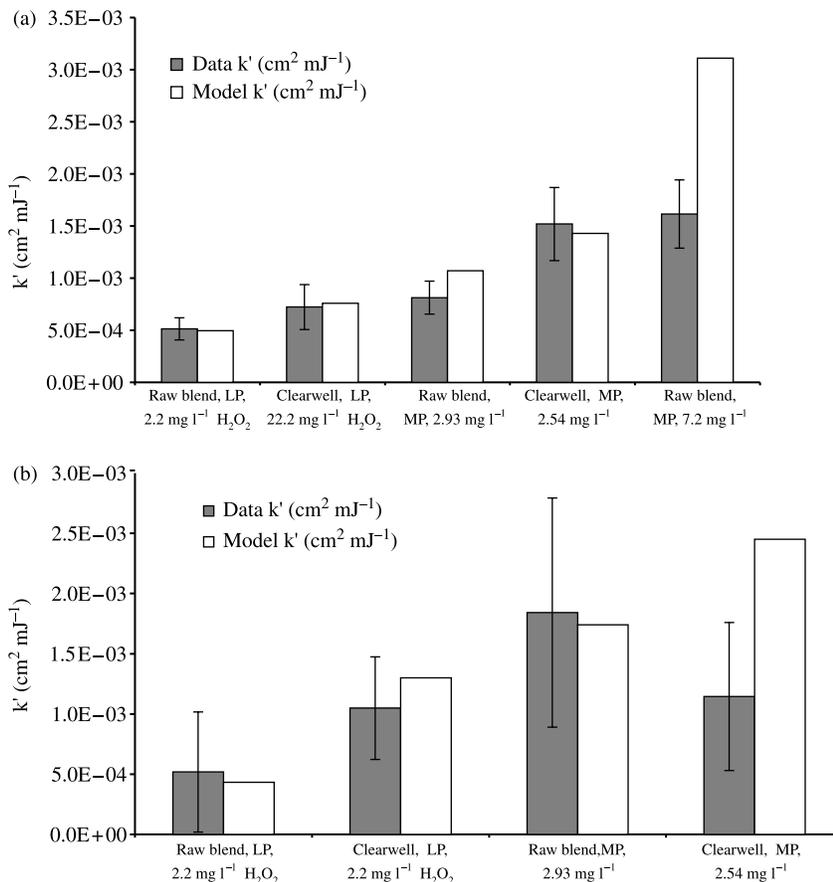

Figure 6 │ Comparison of model predicted and observed fluence-based pseudo-first order rate constant k′ ($cm^2 \, mJ^{-1}$) with 95% confidence intervals for MIB (a) and geosmin (b).

independently verified using an OH radical probe. Another explanation for the variability in the observed rate constants is the low spiking concentrations ($\sim 2\text{--}5$ times the minimum detection limit), which could have increased the error associated with the measured rate constants. The model has been used previously to accurately predict destruction of many contaminants in natural waters at high initial concentrations (Glaze *et al.* 1995; Rosenfeldt & Linden 2004), and in this case, the model over-predicts by less than 50% in each case, so the model should still be regarded as a valid and simple way to predict destruction of MIB and geosmin in clearwell and raw blend water.

Electrical energy per order (E_{EO})

Electrical energy per order (E_{EO}) is defined as the electrical energy (in kilowatt hours) required to decrease the concentration of a target contaminant in 1,000 US gallons (3,785 liters) of water by one order of magnitude. This figure of merit is very specific regarding reactor geometry, UV lamp, contaminant and water quality. However, by utilizing fluence-based reaction kinetics determined in a given water quality, an E_{EO} for a reactor of known geometry and UV lamp can be accurately determined (Bolton and Stefan 2002).

By using the fluence-based kinetic parameters presented above, an E_{EO} was modelled for these waters in a cylindrical 38 liters batch reactor. The reactor modelled is described as a vertical cylindrical reactor, with a volume of 38 liters, radius 35 cm and quartz sleeve radius 6.8 cm. A 1 kW medium pressure UV lamp is mounted in the centre of the reactor, and

operated at half power. For the LP system, the equivalent of four 60 W lamps, operating at full power, is modelled. These reactor dimensions were chosen in accordance with the reactor used by Andrews *et al.* (1995), who found E_{EO} values for UV/H₂O₂ oxidation of geosmin in Grand River water. By modelling the same reactor, the data from this study can be compared with the Andrews *et al.* values.

The average irradiance in the modelled reactor was calculated using the computer program UVCalc (Bolton Photosciences Inc., Edmonton, Alberta, Canada), with inputs of clearwell and raw blend water transmittances at each peroxide level, reactor size, lamp efficiency (15% for MP lamp and 30% for LP lamps) and power of lamps (0.5 kW assuming one MP lamp operated at half power and 240 W assuming four LP lamps operated at full power). The average irradiance values obtained from UVCalc are displayed in Table 3.

By inputting the reactor parameters, fluence-based rate constant values, and the calculated average irradiance numbers into Equation (6), an E_{EO} can be determined for treatment of MIB and geosmin by the UV + H₂O₂ AOP.

$$E_{EO} = \frac{0.6396\,P}{Vk_1'E_{avg}'} \tag{6}$$

where P is the power of the lamp (kW), V is the volume of treated water (l), k' is the fluence-based pseudo-first order rate constant (cm² mJ⁻¹), and E_{avg}' is the UV fluence rate throughout the reactor (mW cm⁻²).

Figure 7 displays the E_{EO} for treatment of MIB and geosmin in each water type using direct UV and UV + H₂O₂ AOP. Due to the specific nature of E_{EO} values, the trends of the parameter are more important than the absolute values

Table 3 | UV fluence rate (E') as calculated by UVCalc in each water. Percentage transmittance is for a 1 cm pathlength and is calculated as a lamp emission weighted average from 200–300 nm for MP experiments, and at 254 nm for LP experiments

Water	MP			LP		
	H₂O₂ (mg l⁻¹)	% Trans (200–300 nm)	E' (mW cm⁻²)	H₂O₂ (mg l⁻¹)	% Trans (254 nm)	E' (mW cm⁻²)
Raw blend	0	92.9	7.91	0	95.1	9.28
Raw blend	2.30	92.5	7.72	2.20	94.8	9.03
Raw blend	7.20	91.8	7.3	n/a	n/a	n/a
Clearwell	0	96.3	10.8	0	97.5	11.8
Clearwell	2.93	95.4	9.94	2.54	97.2	11.4
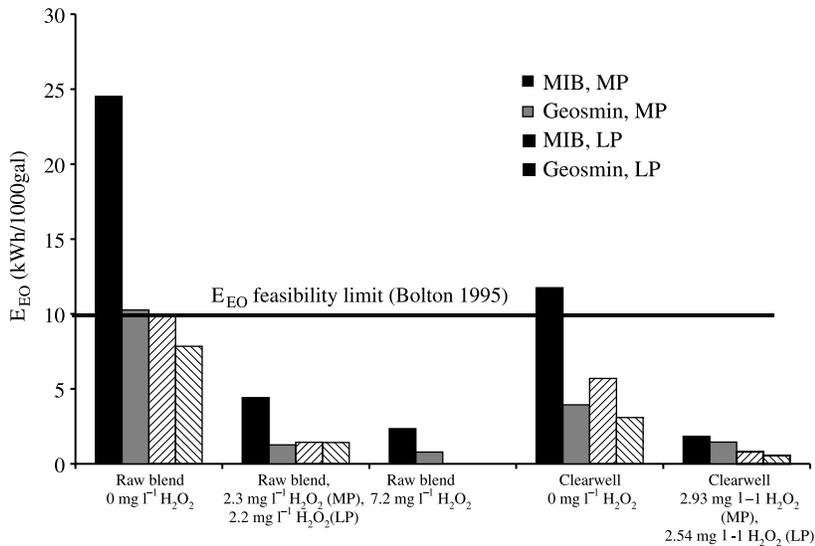
Figure 7 │ Comparison of electrical energy per order values for the destruction of MIB and geosmin in raw blend and clearwell water, calculated using the fluence-based rate constants found in this work, modelled using the reactor specifications from Andrews *et al.* (1995) (1000 US gallons = 3,785 liters).

themselves. The calculated E_{EO} values in Figure 7 show that, for the Chicago waters, a significant reduction in the UV energy needed to treat MIB and geosmin is achieved with the addition of hydrogen peroxide. Assuming an electricity cost of US$.075 per kilowatt hour, an E_{EO} of 10 kWh per 1,000 gallons (3,785 liters) corresponds to a treatment cost of US$0.75 per 1,000 gallons (3,785 liters) to reduce the contaminants by one order of magnitude. This cost considers only the cost of electricity needed to run the lamps, and neglects the costs associated with the hydrogen peroxide addition.

Andrews *et al.* (1995) found that treating geosmin in Grand River water using an MP lamp at 0.5 kWh in the above modelled reactor yielded E_{EO} values of 30.3 for direct UV destruction, 13.8 for UV + 5 mg l^{-1} H$_2$O$_2$, and 4.51 for UV + 25 mg l^{-1} H$_2$O$_2$. In the inlet Chicago water, the addition of only 2.9 mg l^{-1} H$_2$O$_2$ yielded an E_{EO} value equivalent to or less than UV + 25 mg l^{-1} H$_2$O$_2$ in Grand River water.

CONCLUSIONS

UV and UV + H$_2$O$_2$ processes can destroy difficult to remove taste and odour compounds such as MIB and geosmin, but at significantly greater UV fluences than are customarily used for UV disinfection. For direct UV treatment, MP UV is more effective than LP UV, attributed to the polychromatic nature of the emission spectrum of MP

lamps compared with the monochromatic emission of the LP lamp. Additionally, water quality parameters such as turbidity negatively affect UV treatment.

Addition of hydrogen peroxide to the UV processes creates advanced oxidation, and increases the rates of MIB and geosmin destruction in raw blend and clearwell water. Water quality affects the UV + H$_2$O$_2$ oxidation of MIB and geosmin, as destruction in clearwell water was consistently faster than in raw blend water.

The steady state OH radical model can predict destruction of MIB and geosmin in both raw blend and clearwell water at low H$_2$O$_2$ concentrations. This model provides a useful tool in estimating destruction of MIB and geosmin based on water quality parameters such as alkalinity, TOC, pH and UV absorbance. This tool can be used to aid in the design of UV systems implemented in treatment plants over a range of input water parameters, although for MP systems with elevated peroxide addition, the model may over-predict destruction.

Electrical energy per order calculations were performed for a specific reactor geometry and lamp properties and compared with published E_{EO} values. The E_{EO} values calculated from the work performed in this study were lower than previously reported, indicating that water quality issues play an important role in determining the electrical cost feasibility of a UV/H$_2$O$_2$ process for destroying MIB and geosmin.

REFERENCES

Andrews, S. A., Huck, P. M., Chute, A. J., Bolton, J. R. & Anderson, W. A. 1995 UV oxidation for drinking water: Feasibility studies for addressing specific water quality issues. *AWWA Water Quality and Technology Conference, New Orleans, Louisiana*, November 12–16.

Baxendale, J. H. & Wilson, J. A. 1957 The photolysis of hydrogen peroxide at high light intensities. *Trans. Faraday Soc.* **53**, 344–356.

Bolton, J. R. & Linden, K. G. 2003 Standardization of methods for fluence (UV dose) determination in bench-scale UV experiments. *J. Environ. Engng* **129**(3), 209–215.

Bolton, J. R. & Stefan, M. I. 2002 Fundamental photochemical approach to the concepts of fluence (UV dose) and electrical energy efficiency in photochemical degradation reactions. *Res. Chem. Intermediates* **28**(7–9), 857–870.

Bruce, D., Westerhoff, P. & Brawley-Chesworth, A. 2002 Removal of 2-methylisoborneol and geosmin in surface water treatment plants in Arizona. *J. Wat. Suppl.: Res. & Technol. – AQUA* **51**(4), 183–197.

Buxton, G. V., Greenstock, C. L., Helman, W. P. & Ross, A. B. 1988 Critical-reviews of rate constants for reactions of hydrated electrons, hydrogen-atoms and hydroxyl radicals (OH/O$^-$) in aqueous-solution. *J. Phys. Chem. Ref. Data* **17**(2), 513–886.

CDWM (Chicago Department of Water Management) 2002 *Annual Water Quality Report*. Chicago Department of Water Management, Chicago, Illinois.

Crittenden, J. C., Hu, S. M., Hand, D. W. & Green, S. A. 1999 A kinetic model for H2O2/UV process in a completely mixed batch reactor. *Wat. Res.* **33**(10), 2315–2328.

Crozes, G., Hagstrom, J., Suffet, I. H. & Young, C. 1999 Bench-scale evaluation of adsorptive processes for taste and odours control using rapid small-scale column tests and flavor profile analysis. *Wat. Sci. Technol.* **40**(6), 39–44.

Ferguson, D. W., McGuire, M. J., Koch, B., Wolfe, R. L. & Aieta, E. M. 1990 Comparing peroxone and ozone for controlling taste and odour compounds, disinfection by-products, and microorganisms. *J. Am. Wat. Wks Assoc.* **82**(4), 181–191.

Gillogly, T. E. T., Snoeyink, V. L., Newcombe, G. & Elarde, J. R. 1999 A simplified method to determine the powdered activated carbon dose required to remove methylisoborneol. *Wat. Sci. Technol.* **40**(6), 59–64.

Glaze, W. H., Schep, R., Chauncey, W., Ruth, E. C., Zarnoch, J. J., Aieta, E. M., Tate, C. H. & McGuire, M. J. 1990 Evaluating oxidants for the removal of model taste and odor compounds from a municipal water supply. *J. Am. Wat. Wks Assoc.* **82**(5), 79–84.

Glaze, W. H., Lay, Y. & Kang, J. W. 1995 Advanced oxidation processes: A kinetic model for the oxidation of 1,2-dibromo-3-Chloropropane in water by the combination of Hydrogen-peroxide and UV-radiation. *Ind. Engng Chem. Res.* **34**(7), 2314–2323.

Hargesheimer, E. E. & Watson, S. B. 1996 Drinking water treatment options for taste and odor control. *Wat. Res.* **30**(6), 1423–1430.

Huck, P. M., Kenefick, S. L., Hrudey, S. E. & Zhang, S. 1995 Bench-scale determination of the removal of odour compounds with biological treatment. *Wat. Sci. Technol.* **31**(11), 203–209.

Klassen, N. V., Marchington, D. & McGowan, H. C. E. 1994 H$_2$O$_2$ determination by the I$_3^-$ method and by KMNO$_4$ titration. *Analyt. Chem.* **66**(18), 2921–2925.

Koch, B., Gramith, J. T., Dale, M. S. & Ferguson, D. W. 1992 Control of 2-methylisoborneol and gesomin by ozone and peroxone: a pilot study. *Wat. Sci. Technol.* **25**(2), 291–298.

Lalezary, S., Pirbazari, M. & McGuire, M. J. 1986 Oxidation of five earthy-musty taste and odor compounds. *J. Am. Wat. Wks Assoc.* **78**(3), 62–69.

Larson, R. A. & Zepp, R. G. 1988 Reactivity of the carbonate radical with aniline derivatives. *Environ. Toxicol. Chem.* **7**(4), 265–274.

Lawton, L. A., Robertson, P. K. J., Robertson, R. F. & Bruce, F. G. 2003 The destruction of 2-methylisoborneol and geosmin using titanium dioxide photocatalysis. *Appl. Catalysis B – Environ.* **44**(1), 9–13.

Liu, W. J., Andrews, S. A., Stefan, M. I. & Bolton, J. R. 2003 Optimal methods for quenching H$_2$O$_2$ residuals prior to UFC testing. *Wat. Res.* **37**(15), 3697–3703.

Mamane-Gravetz, H. & Linden, K. G. 2004 Impact of particle-aggregated microbes on UV disinfection proceedings. *AWWA Water Quality Technology Conference*, San Antonio, Texas, 14–17 November 2004.

Notre Dame Radiation Laboratory Chemistry Data Center, www.rcdc.nd.edu/Solnkin2/ 1 December 2004.

Rosenfeldt, E. J. & Linden, K. G. 2004 Degradation of endocrine disrupting chemicals bisphenol A, ethinyl estradiol, and estradiol during UV photolysis and advanced oxidation processes. *Environ. Sci. Technol.* **38**(20), 5476–5483.

Sharpless, C. M. & Linden, K. G. 2003 Experimental and model comparisons of low- and medium-pressure Hg lamps for the direct and H$_2$O$_2$ assisted UV photodegradation of N–Nitrosodimethylamine in simulated drinking water. *Environ. Sci. Technol.* **37**(9), 1933–1940.

Suffet, I. H., Corado, A., Chou, D., McGuire, M. J. & Butterworth, S. 1996 AWWA taste and odor survey. *J. Am. Wat. Wks Assoc.* **88**(4), 168–180.

Suffet, I. H., Khiari, D. & Bruchet, A. 1999 The drinking water taste and odor wheel for the millennium: beyond geosmin and 2-methylisoborneol. *Wat. Sci. Technol.* **40**(6), 1–13.

Wells, C. J. H. 1972 *Introduction to Molecular Photochemistry*. Chapman and Hall, London.